JOURNAL OF MATERIALS SCIENCE 11 (1976) 1927–1938

Low temperature dynamic mechanical response of porous Vycor glass as a function of moisture content

Part 1 *The capillary transition*

ERIK J. SELLEVOLD
Building Materials Laboratory, Technical University of Denmark, Lyngby, Denmark

FARIBORZ RADJY
Geomat Consulting Engineers, Kh. Mehrshah, (Apadana), Kh. Niloufar, No. 70 K. Nastarin, Tehran, Iran

An experimental apparatus designed to measure automatically the internal friction and the elastic modulus of solid beams based on the resonance principle is described. The internal friction and the elastic modulus of porous Vycor glass beams containing different amounts of water has been measured as a function of temperature from 25 to −160° C. Two transitions are evident in the response: the capillary transition (−40 to 0° C) caused by freezing of capillary condensed water, and the adsorbate transition (centred around −85° C) associated with a gradual solidification of water adsorbed near the pore surfaces. More than half of all the water in a saturated beam freezes during the capillary transition, but this ice contributes only modestly to the elastic modulus of the beam which implies that there is little contact between the ice and the glass matrix. Further cooling into the adsorbate transition temperature range is believed to cause a gradual solidification of the adsorbed water, until at very low temperatures the adsorbed layer is "glassy" and effectively cements the glass matrix and the ice together resulting in a large increase in the elastic modulus of the beam.

1. Introduction

Since the early 1940s measurements of the dynamic mechanical response (DMR) – elastic modulus E and internal friction $\tan\delta$ – of various materials systems (crystalline solids and glasses [1], polymers [2]) have played an important role in elucidating structure–property relationships in these materials. Such measurements become useful mainly if the DMR response spectrum (as a function of temperature or frequency) shows transitions, i.e. $\tan\delta$ peaks and modulus transitions.

Work undertaken at Stanford University since 1964 led to the discovery [3,4] of two marked transitions in the DMR of hardened cement paste (the binder phase in concrete) as a function of temperature. From the very beginning it was realized that these transitions were associated with adsorbed and capillary condensed water in the micropores of hardened cement paste. The transitions were therefore named as follows: the "adsorbate" transition (near −90° C), and the "capillary" transition (−40 to 0° C). The work on hardened cement paste was continued by Helmuth [5]. In 1971 we began a project in this laboratory in order to ascertain if the transitions observed previously are general phenomena existing in any substance that adsorbs water, or are peculiar to hardened cement paste. The results [6,7] showed that the transitions do indeed exist in such diverse,

water adsorbing materials as wood, silica gel, porous Vycor glass, clay and possibly alumina.

The existence of these transitions makes, for the first time, the DMR technique a useful tool in a new class of materials in conjunction with hitherto unexplored types of processes. The purpose of our continuing project is to utilize the two transitions to explore structure–property relationships in water adsorbing substances. Our main motivation for this interest is that most non-metallic building materials, being porous, adsorb appreciable amounts of moisture which, in turn, modifies almost all of their important engineering properties. At the same time these investigations – in conjunction with the use of other techniques such as NMR – may lead to a better understanding of the structure of adsorbed water, in itself a fundamentally interesting and important problem.

In the present article we describe the experimental apparatus, and report DMR results for porous Vycor glass containing different amounts of adsorbed water. Only the capillary transition will be discussed here – discussion of the adsorbate transition follows in Part 2 of this paper.

2. Experimental aspects

2.1. Measurement technique

The porous Vycor glass (PVG) was supplied by Corning Glass Co. in the form of slender beams ~200 mm long, 8 mm wide and 4.4 mm deep. The beams are supported at their nodal points on thin wires, and are vibrated in a free-free mode. The E-modulus and the internal friction are computed using the following equations:

$$\tan\delta = \frac{f_h - f_l}{f_r}, \qquad E = C\frac{f_r^2 \cdot m \cdot L^4}{I} \qquad (1)$$

where f_r = resonance frequency; f_h = upper 3 dB frequency; f_l = lower 3 dB frequency; C = constant depending on mode of vibration; m = mass per unit length of beam; L = length; I = moment of inertia.

Fig. 1 shows the specimen support system and the cooling oven. In order to minimize moisture losses during cooling, the specimen is placed inside a small plexiglass chamber which is sealed with teflon tape. The chamber contains movable wire supports for the specimen and a small platinum

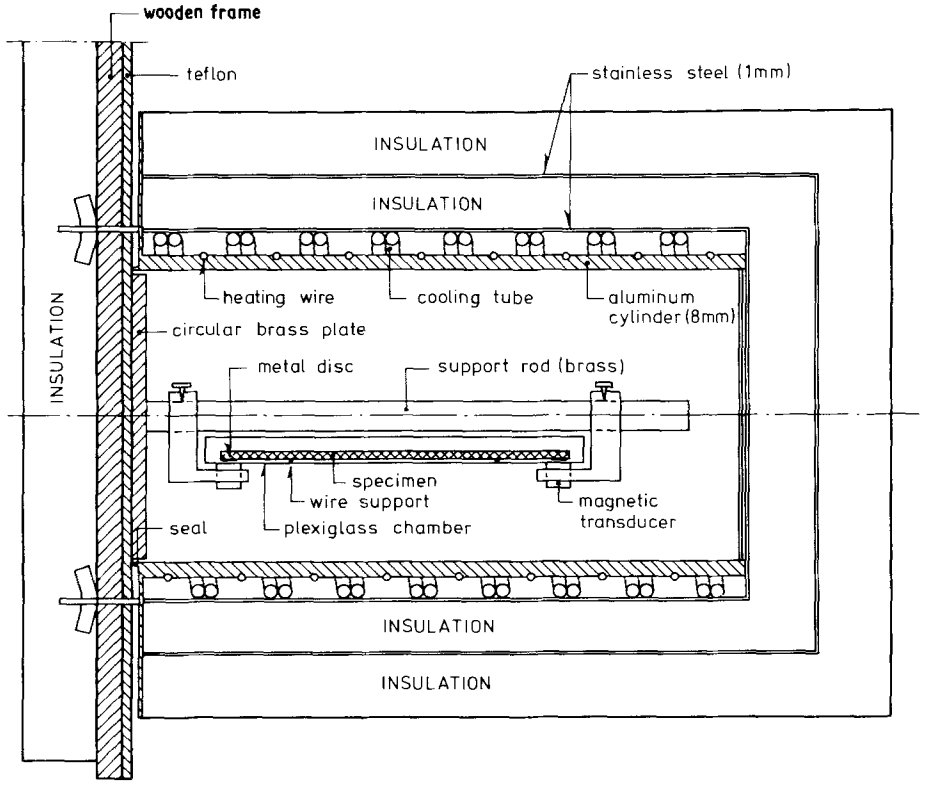

Figure 1 Cooling oven with specimen support system.

resistance temperature sensor close to the centre of the beam. The temperature sensor is operated via a signal conditioner in the datalogger, enabling direct four digit display on the digital indicator in degrees centigrade to a resolution of 0.1° C.

The plexiglass chamber is clamped to the top of two magnetic transducers (one for excitation and one for detection. Metal clips clipped on the ends of the specimen couple the specimen to the transducers. The plexiglass chamber and the transducers are attached to a circular brass base plate via a horizontal cylindrical brass rod. The base plate is, in turn, screwed to a wooden frame. In order to minimize the transmission of mechanical vibrations, a teflon plate is inserted between the base plate and the supporting wood frame. The whole assembly is supported by a rigid brick wall via the wooden frame. The cylindrical oven is suspended from an overhead rail so that it can be opened and closed by a smooth sliding action. In a closed position (Fig. 1), a knife-edge on the inner Al-cylinder is forced against a groove in the teflon plate, thus sealing the oven chamber. The electrical wires are taken out via a vacuum leadthrough. This support system was found to isolate the specimen very effectively from external mechanical shocks.

2.2. Temperature control

Programmed cooling and heating are obtained by controlling the flow of liquid nitrogen through a 20 m (8 mm) long copper tube built into the oven (Fig. 1). The nitrogen tank (50 litre capacity) outlet is connected to one end of the cooling coil, while a solenoid valve followed by a throttling valve is attached to the other end. A standard temperature controller-programmer designed for heating is used with a platinum resistance sensor imbedded in the heavy Al-cylinder. The output of the temperature controller-programmer is first reversed by a relay and then used to drive the solenoid valve. One tank of liquid nitrogen was sufficient for a standard run to −160° C.

2.3. Electronic equipment

In line with the usual practice, the electronic equipment for exciting and detecting the vibrations consists of an oscillator, a frequency counter, a voltmeter and a digital voltmeter. However, our apparatus has the less usual feature of being capable of operating in an automatic mode. The Brüel & Kjaer Company, Copenhagen, constructed for us a special unit (Model 5627) which in conjunction with the other standard components has the following capabilities:

(1) starting from a preselected reference frequency, it enables the oscillator to sweep the frequency spectrum while monitoring the amplitude in order to detect f_r, f_h and f_l;

(2) f_r, f_h and f_l are stored in three separate memories, and a new sweep is automatically initiated after a 5 sec pause at the frequency f_l;

(3) the register can be read out either by manual triggering or by a clock-initiated signal from the datalogger.

In this manner the apparatus continually tracks the resonance frequency f_r, as well as the two side frequencies f_h and f_l. The sweep rate can be varied from 0.05 to 16 Hz sec^{-1}; it is usually set such that one sweep through the bandwidth $(f_h - f_l)$ takes a minimum of 20 sec. Most experiments are run at a frequency between 300 to 1600 Hz with a resolution of 0.1 Hz. A typical test usually takes up to 48 h, and involves up to 400 readings at less than 1° C intervals. The computer output lists time, temperature, f_r, f_h, f_l, $\tan\delta$, E and per cent E change relative to the reference value at room temperature. Plots are also produced as functions of time and temperature.

3. Specimen preparation and characterization

Two companion beams, PVG4 and PVG5, were tested extensively in the DMR apparatus. The beams were slightly discolored (brownish) when received. An unsuccessful attempt to clean them by washing in solvents was followed by oven heating at 500° C for 1 week which completely cleaned the beams. After the heat cleaning, the beams were placed in a vacuum desiccator over a salt solution (relative vapour pressure = 0.32), then in water at 98° C for 1 day. Finally, they were dried at a pressure of about 10^{-5} Torr at 26.8° C and weighed. These dry weights were about 1% higher than those found immediately after the 500° C oven cleaning.

One of the beams, PVG4, was then tested in the DMR apparatus four times, each time at a different equilibrium moisture content. However, the beam again became discolored and the 500° C cleaning procedure was repeated, followed by drying at 1.25×10^{-4} Torr (26.8° C). Both the sorption and the DMR experiments made after the second cleaning reproduced those made after the first cleaning. The two beams were moisture conditioned

TABLE I Porous Vycor glass properties

Property	PVG4	PVG5
Saturated water content g/g dry PVG	0.2255	0.2274
Porosity (assuming water density = 1.0)	0.3307	0.3316
Porosity (assuming solid glass density = 2.182)	0.3281	0.3318
BET surface area (water)	$89\ m^2\ g^{-1}$	
BET surface area (nitrogen)	$188\ m^2\ g^{-1}$	

in vacuum desiccators before the DMR runs: at relative vapour pressures below 0.75 by placing them over saturated salt solutions; at higher moisture contents by simply introducing the desired amount of water into the desiccator. The saturated weight was found by weighing the beams in a saturated surface dry (SSD) condition after they had been immersed in water under vacuum.

A solid Vycor glass beam (Corning no. 7913) was also tested in the DMR apparatus. The volumes and weights of both solid and dry porous beams were determined. The porosity of the two porous beams were then calculated two ways: (1) by using the SSD and dry bulk densities assuming the pore-water to have a density equal to unity, (2) by using the solid density found for the solid beam (2.182 $g\,cm^{-3}$) and the bulk dry densities of the porous ones. The results are given in Table I.

Two beams from the same batch as PVG4 and PVG5 were cleaned once as described above, crushed and sieved. The grain size was between 0.25 and 0.149 mm. A series of sorption isoteres between 25 and 95° C, covering the moisture range from dry to saturated, were made using this powder. (Complete results from these experiments will be published by Radjy [8].) Fig. 2 shows the sorption isotherm at 25° C constructed from the isostere data. Fig. 2 also demonstrates very good agreement between the adsorption curves for powder and beams. The BET surface area was calculated using the adsorption data in Fig. 2 based on a molecular area for water of 11.4 $Å^2$. The nitro-

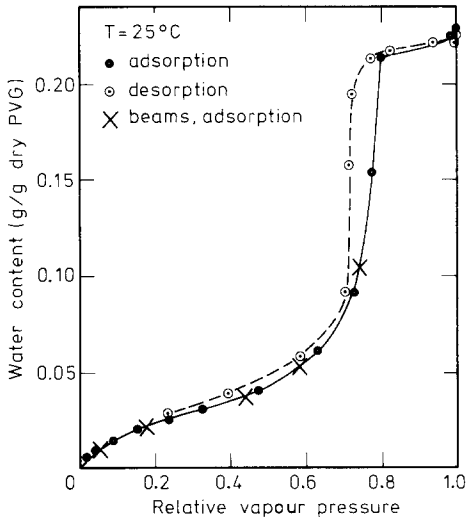

Figure 2 Sorption isotherms for porous Vycor glass.

TABLE II Parameters and results of DMR runs

Run no.		Water content* (%)	ΔW† (%)	At start of tests‡			After tests‡
PVG4	PVG5			E(RT) × 10^{-5} ($kgf\,cm^{-2}$)	tan δ (RT) (%)	f_r(RT) (Hz)	E (RT) × 10^{-5} ($kgf\,cm^{-2}$)
	1 (s)	dry	+ 0.41	1.738	0.07	850.3	1.731
2		dry	+ 0.23	1.817	0.06	403.4	1.816
	3	1.17	+ 0.19	1.773	0.15	396.7	1.775
	4	2.21	+ 0.09	1.785	0.13	396.0	–
	5	3.64	0	1.797	0.15	394.7	–
	6	5.28	− 0.28	1.797	0.15	391.5	1.797
	7	9.99	− 0.62	1.801	0.16	383.8	1.804
12 (s)		12.70	− 0.17	1.847	0.16	420.2	1.850
	8	14.29	− 0.12	1.808	0.16	377.3	1.809
	9	19.48	− 0.12	1.817	0.16	370.1	1.793
10		19.53	− 0.23	1.894	0.16	377.6	1.896
11		22.55	− 0.61	1.950	0.26 0.16	378.5	1.951

* Per cent of dry beam weight.

† Water content after test minus water content before test.

‡ RT = room temperature.

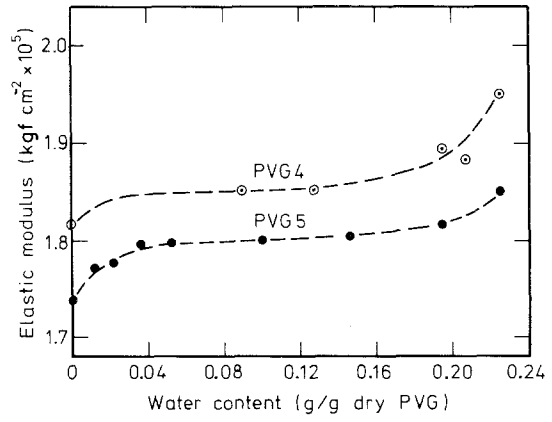

Figure 3 Room temperature E-moduli of two porous Vycor glass beams as a function of water content.

gen surface area was found using a Perkins-Elmer Sorptomat and a one point determination. The BET surface areas are listed in Table I.

4. DMR results

Table II assigns DMR run identification numbers and lists a number of test parameters and results for the DMR runs on the two beams PVG4 and PVG5. The rate of temperature change was about $12^\circ\,Ch^{-1}$ during cooling and about $9^\circ\,Ch^{-1}$ during heating. The heating rate was slower above -70° C, since in this temperature range the natural heating rate was smaller than the $9^\circ\,Ch^{-1}$ set on the controls. The beams were weighed before and after each test; the differences in moisture contents are listed in Table II. These values do not vary entirely systematically with the initial moisture contents, probably because the time a specimen was left in the apparatus after completion of a run varied considerably.

Test 9 resulted in cracks at one end of PVG5, caused by too fast cooling. Table II shows that the cracks reduced the room temperature elastic modulus. The cracked end was subsequently cut off, and one more run (run no. 1) indicated by S (for short) made with PVG5. Runs 10 and 11 were made with cooling rates of $1.8^\circ\,Ch^{-1}$ down to about -45° C, without causing damage to the specimen.

The initial room temperature E-modulus, $E\,(RT)$, values as a function of moisture content are plotted in Fig. 3. Table II lists initial $\tan\delta$ values at room temperature. The dry beams show less damping than moist ones. The value of 0.06% is the same as that found for materials with practically zero damping; 0.06% therefore represents damping inherent in the system. The saturated run (no. 11) has two initial damping values listed; the first one is the room temperature value, the second lower value represents a plateau value reached before nucleation starts. This decrease in damping is probably associated with moisture loss.

The elastic modulus change during cooling for various moisture contents is shown in Fig. 4. The response of the solid Vycor glass beam is also shown. It has the unusual feature that the Elastic modulus decreases with decreasing temperature. Corning Glass Co. gives E-values from 25 to 800° C. Linear extrapolation of their data from 25 to -160° C predicts a loss in E-modulus of 3%, a

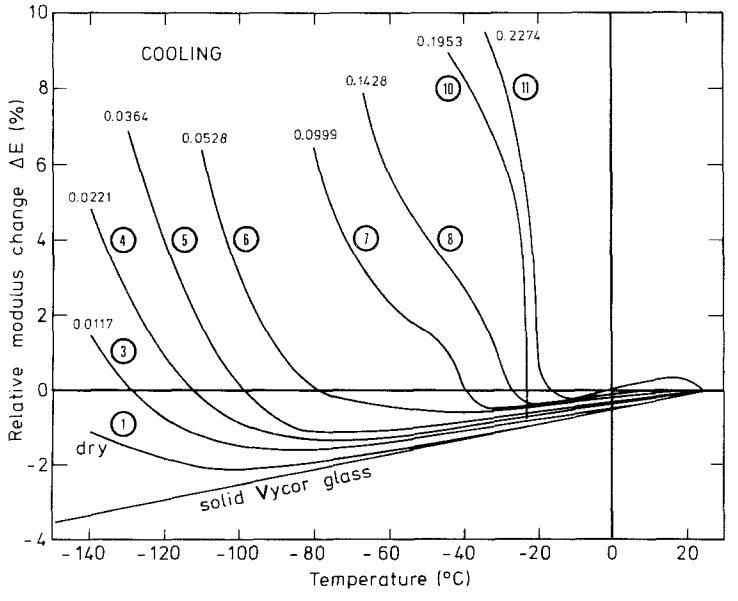

Figure 4 Relative modulus change during cooling of porous Vycor glass beams. Decimal numbers give water content g/g dry glass. Circled numbers identify run no. in Table II.

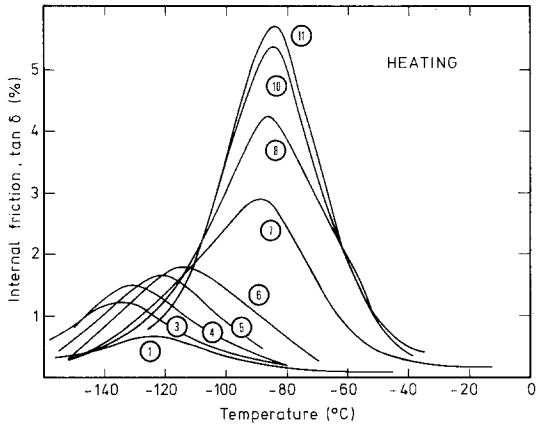

Figure 5 Internal friction during heating of porous Vycor glass beams with different water contents. Circled numbers identify run no. in Table II.

figure reasonably close to our experimental value of 3.6%.

Internal friction and elastic modulus change curves obtained during heating are drawn in Figs. 5 and 6. Solid lines represent experimental data; the dotted lines are extrapolations. As was usual, a perfectly smooth line can be drawn through the experimental points from each run; points are therefore not shown. The tan δ curves (Fig. 5) are not drawn up to room temperature. The curves are essentially flat; even at high moisture contents there is only a very small tan δ peak associated with the capillary transition.

Fig. 7 shows the ΔE–T curves (cooling and heating) for run no. 12 with a cooling rate of $2^\circ\,C\,h^{-1}$ and a heating rate above -30° C of $1^\circ\,C\,h^{-1}$.

5. Discussion and conclusions: the capillary transition

5.1. Length change data – DMR data

Calorimetric, DTA, length change and sorption measurements on the system PVG-water, at temperatures below 0° C, have been made by a number of workers. Here we will briefly review the results most relevant to the present study. Litvan [9] measured a "cooling–warming" length change isostere (simultaneously with a thermogram) on a saturated PVG beam (T-rate = $1.25^\circ\,C\,h^{-1}$). His results and interpretation were briefly as follows: freezing initiated at -6° C and was accompanied by a small contraction. Litvan concludes that the ice forms on the outside surface of the specimen; the contraction is caused by desorption from the specimen to the ice. Further cooling leads to more desorption to the ice phase and more contraction of the glass. At -18° C a strong expansion starts, associated with solidification of water in the pores. We refer to this transition as the capillary transition. The expansion continues to about -30° C; from -30° C to -45° C very little dilatation takes place. Heating from -45° C produces the same two transitions; the capillary transition is complete at

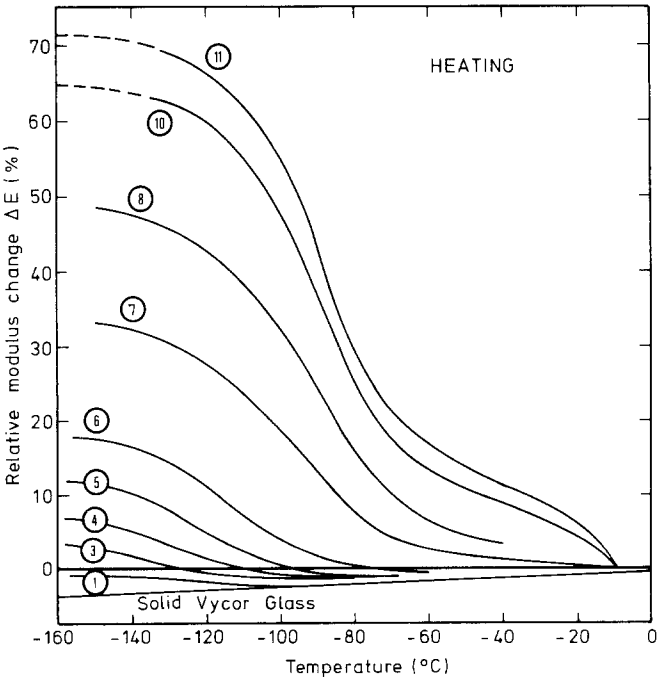

Figure 6 Relative modulus change during heating of porous Vycor glass beams with different water contents. Circled numbers identify run no. in Table II.

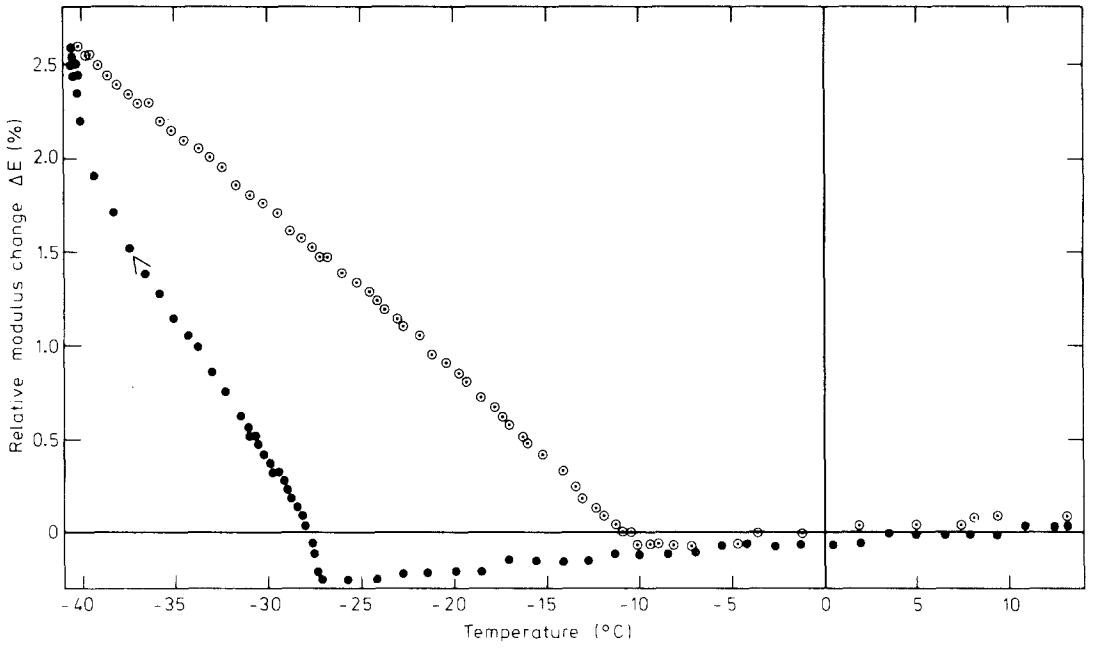

Figure 7 Relative modulus change during slow cooling and heating of a porous Vycor glass beam. Run no. 12 (Table II). Water content 0.127 g/g. Cooling rate = 2° C h^{-1}. Heating rate = 1° C h^{-1}.

about −10° C, the surface ice phase melts at 0° C. The length changes are about the same during heating as during cooling, i.e. the specimen returns to its original length. The rate of temperature change has an important influence on the results. Faster cooling rates produce much greater expansion during the capillary transition and result in permanent expansion of the specimen after a completed run. Very slow rates (2° C day^{-1}) result in less expansion during the capillary transition, and the marked capillary transition is absent during heating, i.e. the specimen expands gradually until it reaches the original dimensions at about −4° C. The main features of Litvan's cooling–warming isosteres have been found also by Antonieu [11] and Feldman [12].

The elastic modulus data in Fig. 4 show a well-defined nucleation temperature for moisture contents of 10% or more. The abrupt increase in elastic modulus clearly corresponds to the expansion observed in the length change experiments, both in our opinion being manifestations of ice formation in the pores. Different investigators [9, 11, 12] have reported nucleation temperatures for saturated specimens ranging from −14 to −24° C, our value being about −20° C. These differences are not surprising since the cooling rates employed differed, and furthermore, it is clear from the extensive literature that the properties (sorption isotherms and BET surface areas) of different PVGs are not identical.

The cooling–heating hysteresis associated with the capillary transition is most clearly shown in Fig. 7. The highest melting temperature of about −9° C (Fig. 6) agrees with Litvan's results [9].

5.2. Weight loss during cooling

Litvan [9] and Feldman [12] both concluded that cooling of a saturated specimen led to desorption and ice formation in the chamber or on the surface of the specimen. Antonieu [11], on the other hand, found that a cooling rate of less than 2° C h^{-1} and the presence of 25 Torr helium pressure in the vacuum chamber effectively prevented moisture losses during cooling of a saturated specimen. In our case the specimen was surrounded by atmospheric pressure, and, for the two highest moisture contents, the cooling rate was less than 2° C h^{-1}. Table II shows that even so the specimen lost a small amount of moisture during the test. The numbers in Table II represent minimum values for moisture losses, since any water distilled out to an external ice phase during cooling could be adsorbed back into the specimen during heating, and thus not be recorded as a weight change. We made a separate experiment to measure weight loss: a saturated specimen was placed in a thin-walled glass tube with a stopper and placed on top of the

plexiglass specimen chamber in the cooling oven. The oven was cooled at 1.8° C h^{-1} and opened up quickly at about −25° C (below the nucleation temperature of −20° C, Fig. 4). Ice had formed on the inside surface of the glass tube, but none could be seen on the specimen surface. The specimen was transferred to another glass tube, and both tubes weighed. The weight gain of the original tube corresponded with the weight loss of the specimen, both amounting to about 0.5% based on the dry weight of the specimen. The experiment was repeated and the result reproduced. The 0.5% weight loss is about the same as the total weight change during the test (Table II). It seems unlikely that further cooling should produce substantial weight losses since at −25° C the larger pores are already blocked with ice.

Our estimate of the weight loss does not contradict Litvan and Feldman's explanation of the contraction down to −20° C. The amount of moisture loss needed to cause the contraction observed by them can be estimated from their length change–sorption isotherm and is smaller than 1.0%. Further evidence supporting our estimate of the cooling weight loss is afforded by the $\Delta E-T$ curves in Fig. 4. For the saturated specimen the initial cooling produced an apparent increase in E of about 0.4%. This apparent increase is most probably caused by a weight loss, which according to Equation 1 increases the resonance frequency, and therefore is recorded as an increase in E. The weight loss necessary to produce an apparent increase in E of 0.4% is about 0.4% of the beam dry weight – a value which agrees very well with our observed weight loss. We conclude that while moisture loss does take place during cooling of saturated specimens, it is probably less than 1%.

Fig. 4 does not indicate any significant weight losses at moisture contents lower than saturation. Table II also shows very small values for total weight changes during the tests. Litvan [10] measured cooling–length change isosteres at various moisture contents and found the marked contraction down to −20° C (indicating desorption) only for saturated specimens.

5.3. Observed versus theoretical freezing temperatures

Dufay *et al.* [13] have derived a number of approximate equations predicting freezing temperatures for capillary condensed water.

5.3.1. Liquid–vapour interface

Assume that the ice forms at 1 atm pressure, and is not in direct contact with the liquid. This assumption implies that the ice forms in the large pores or outside the specimen and is fed by desorption of the capillary condensed water. The only interfaces present according to this model are a curved liquid–vapour and a flat ice–vapour interface. Dufay *et al.* give the following equation for the freezing point depression:

$$\ln T/T_0 = \frac{2}{\Delta h} \cdot \frac{v^1 \cdot \sigma^{1v}}{R^{1v}} \qquad (2)$$

where T = freezing temperature (K); T_0 = normal triple point temperature (273 K); Δh = heat of fusion; v^1 = molar volume of water; σ^{1v} = surface tension of water; $R^{1v} = r/\cos\theta$ = Kelvin radius of liquid–vapour meniscus; r = radius of a cylindrical pore; θ = contact angle between liquid and pore wall. The relationship between R^{1v} and the relative vapour pressure is given by the Kelvin equation. Using the Kelvin equation and ignoring the temperature variation of Δh, σ^{1v} and v^1 the freezing point depression has been calculated as a function of the relative vapour pressure exerted by the capillary condensed water. The results are shown in Fig. 8 by the curve marked liquid–vapour. The calculation is approximate, but a more rigorous one using the thermodynamic data for the system PVG–water by Radjy [8] gives somewhat larger freezing point depressions since the entropy of the porewater is lower than that of bulk water. The values in Fig. 8 are, however, accurate enough for our purposes. Comparing the theoretical freezing point depressions (Fig. 8) with the temperatures

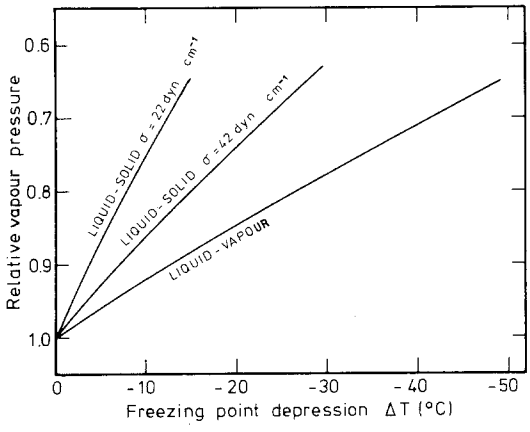

Figure 8 Theoretical freezing point depression of pore water as a function of the relative vapour pressure at which adsorption took place.

at which ice is demonstrated to be present in the poresystem during heating (Fig. 6), there is a large discrepancy. For example, it is clear from the E-modulus curve in Fig. 6 that ice is present at -15° C for a moisture content of 19.53%. However, a moisture content of 19.53% (adsorption) corresponds to $p/p_s = 0.79$ (Fig. 2), and consequently, according to Fig. 8, to a freezing temperature of about -28° C. We conclude that the melting process is not described by this model. Other interface possibilities must be considered to provide consistent interpretations of the experimental results.

During cooling ice formation takes place at about -24° C (Fig. 4) for a moisture content of 19.53%. This temperature is high compared to the theoretical freezing temperature of -28° C, but the discrepancy is much smaller than for the heating results.

5.3.2. Solid–liquid interface

Consider a saturated specimen. Ice forms on the surface under 1 atm pressure, i.e. a flat ice–vapour interface. The pressure, and thereby the chemical potential, of the liquid phase is controlled by the radius of the solid–liquid interface concave toward the liquid. Dufay *et al.* give the freezing point depression for this model:

$$\ln T/T_0 = -\frac{2}{\Delta h} \cdot \frac{v^l \cdot \sigma^{sl}}{R^{sl}} . \qquad (3)$$

Equation 3 predicts smaller freezing point depressions than Equation 2 because σ^{sl} is smaller than σ^{lv}. The value for σ^{sl} is apparently not well established. Dufay *et al.* give a value of 22 dyn cm^{-1}, Everett and Haynes [14] assumed that $\sigma^{sl} = 30$ dyn cm^{-1}. Morioka *et al.* [15] used Equation 3 and a conical pore model to analyse the calorimetric heat capacity data on the system PVG–water obtained by Antonieu [11]. They assumed the heat of fusion for the capillary condensed water to equal that of bulk water. Using a value for σ^{sl} of 42 dyn cm^{-1}, and a pore size distribution function derived from sorption measurements they calculated a heat capacity versus temperature curve that agreed well with Antonieu's experimental one. The strong influence of the σ^{sl} value is demonstrated in Fig. 8, where freezing point depression curves both for $\sigma^{sl} = 42$ and $\sigma^{sl} = 22$ dyn cm^{-1} are drawn. For our saturated test (Fig. 6), the highest temperature at which ice can be detected is about -9° C. Fig. 2 shows that only about 1 wt% water is adsorbed between a relative vapour pressure of 0.8 and unity. About one half of this water is lost during cooling as discussed earlier. If we then, somewhat arbitrarily, assume that the water responsible for the capillary transition in a saturated specimen is that adsorbed at $p/p_s = 0.80$ and that its melting temperature is determined by the solid–liquid interface, Fig. 8 gives an expected melting temperature of -8° C with $\sigma^{sl} = 22$ dyn cm^{-1} 1.

A possible explanation for our observed high maximum melting temperatures and for the cooling–heating hystereses is, therefore, that melting is controlled by the solid–liquid interface while the initiation of freezing is controlled by the liquid–vapour interface.

Fig. 6 shows that the two highest water contents give the same maximum freezing temperature of about -9° C. This implies, therefore, that the freezable water in both cases is associated with the very steep part of the adsorption isotherm (Fig. 2) and that the water adsorbed above $p/p_s = 0.80$ is either lost on cooling or forms ice so placed that it does not contribute to the E-modulus.

5.3.3. More complex models

The simple solid–liquid interface model just discussed appears to us to be unrealistic in connection with specimens in a less than saturated condition, since it is difficult to imagine that ice can exist inside the pore system with a flat ice–vapour interface. If we assume that capillary theory is applicable to water in pores as small as those in PVG, then the only other types of models which can explain the small freezing point depressions observed for our less than saturated specimens are those which predict a chemical potential for the ice phase lower than that of bulk ice, i.e. puts the ice at pressures less than 1 atm. Fig. 9 shows three models which meet this requirement. In type 1 models the tension in the ice phase is imposed by a solid–vapour interface concave toward the vapour. In type 2 models both liquid–vapour and solid–vapour interfaces exist; for the ice to be in tension the pressure drop across the vapour–liquid interface must be greater than the pressure increase across the liquid–solid interface, i.e. $\sigma^{lv}/R^{lv} > \sigma^{sl}/R^{sl}$. In a real system like PVG–water it is, of course, possible for all three situations depicted in Fig. 9 to exist simultaneously.

Morioka *et al.* [15] have applied model 1b to nitrogen and argon adsorption on powdered rutile;

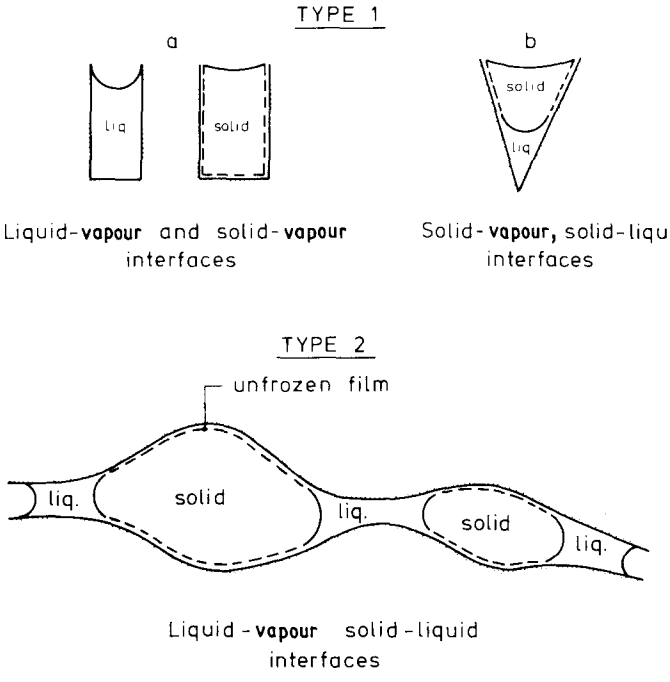

Figure 9 Different configurations whereby solid and liquid can co-exist in pores.

while model 2 has been applied to a number of pore geometries by Everett and Haynes [14]. The additional complications caused by the volume increase associated with the water–ice transformation have not been considered. We will not attempt to apply any of these models quantitatively, but note that either model can, in principle, explain our results in a consistent manner.

5.4. Ice formation and the interaction of ice with the solid matrix

Antonieu [11] calculated that 55% of the water in a saturated PVG sample had frozen at −32° C. His calculation was based on his calorimetric data and the assumption that the heat of fusion of pore water equalled that of bulk water. The same assumption applied to Litvan's calorimetric data [10] gives the result that about 52% of the water in a saturated sample is frozen at −35° C. These values are probably underestimates. The enthalpy of most of the pore water is less than that of bulk water, hence the heat of fusion will be less, provided that the ice is at atmospheric pressure. The pressure dependence of the enthalpy is given by the equation:

$$\left(\frac{\partial H}{\partial p}\right)_T = v^l - T \cdot \left(\frac{\partial v^l}{\partial T}\right)_p \qquad (4)$$

where v^l is the molar volume of water. The Kelvin–Laplace equation gives the tension in capillary condensed water at $p/p_s = 0.77$ as 360 atm. This tension corresponds, by Equation 4, to a decrease in the enthalpy of about 150 cal mol^{-1} or roughly 10% of the heat of fusion. Radjy [8] found the differential enthalpy of adsorbed water at $p/p_s = 0.77$ to be lower than that of bulk water by about 20%. Litvan [11], in interpreting his calorimetric data, assumed that only water in the third and subsequent layers froze, i.e. that 74% of the water in a saturated specimen is frozen at −35° C. A consequence of his assumption is that the corresponding heat of fusion is 30% lower than that of bulk water; a low value compared to Equation 4 and to Radjy's results.

Based on these considerations we accept that at least 50% of the water in a saturated specimen is frozen at −40° C. It is of interest to consider the influence the ice phase has on the E-modulus of the PVG beam. Fig. 6 shows that at −160° C E for a saturated beam has increased by more than 70% over its room temperature value. However, at −40° C, when at least 50% of the water has frozen, the E-modulus has only increased by about 11%. A consistent explanation for this observation is that the ice forms in the centre of the pores and that a film of adsorbed water much less viscous than ice separates the ice from the glass matrix. Further

cooling increases the viscosity of the adsorbed film, until, at very low temperatures (Fig. 6) the adsorbed layer is "glassy" and effectively cements the glass matrix and the ice together.

In contrast to the behaviour of PVG, the capillary transition in hardened cement paste is accompanied by a substantial internal friction peak. The absence of such a peak for PVG is a further indication of weak solid glass–ice interaction in the capillary transition temperature range.

The adsorbate transition, i.e. the gradual increase in viscosity of the adsorbed film, will be discussed in the second part of this paper.

Pearson and Derbyshire [16] made low temperature NMR studies on porous amorphous silicas at different moisture contents. One of their conclusions was that ice formed in the centre of the pores, leaving a mobile adsorbed film between the ice and the pore walls, a view agreeing with our "pea-in-pod" model of ice formation.

The rate of temperature change has a less important effect on the DMR than on the length change behaviour of PVG. Litvan [17] cooled a saturated specimen at $20^\circ\,C\,h^{-1}$ and observed a very large expansion at -21° C, but maintaining the temperature at -21° C for 17 h reduced the expansion considerably. The total expansion at -40° C after further cooling was about the same as that for a similar specimen cooled to -40° C at a rate of $1.25^\circ\,C\,h^{-1}$. We made a similar experiment measuring the E-modulus, but holding the temperature constant below the nucleation temperature simply increased the E-modulus at a decreasing rate until it reached an equilibrium value. Heating the beam stepwise with rates varying from about $5^\circ\,C\,h^{-1}$ (the natural heating rate of the oven) to zero demonstrated that the natural rate gave E–T curves very close to equilibrium, as does the result of the slow cooling–heating run shown in Fig. 7.

The time dependent expansion observed by Litvan is clearly caused by a transport process needed to dissipate pressures generated by the ice formation. It is natural that such pressures should produce dilatation, but not necessarily stiffness increase. The details of the pressure development is not known. The dilatation is, at least not wholly, caused by the 9% expansion accompanying the water–ice transformation. Litvan [9], using PVG, and Beaudoin and MacInnes [18], using hardened cement paste, have shown, using several different adsorbates, that freezing is accompanied by an expansion regardless of the sign of the specific volume change of the adsorbate on freezing in the bulk state. Kipkie *et al.* [19] found the same effect for the system PVG-benzene and suggested it is caused by meniscus destruction upon freezing. In our view, this mechanism alone is not sufficient to explain the sudden and destructive effect of freezing when water is the adsorbate. The pressure causing damage probably is associated with the expansion of water upon freezing, either as localized "hydraulic pressure" in the unfrozen water or as pressure exerted by the ice crystals directly upon the solid matrix. The fact that a slowdown of the cooling rate still results in very rapid ice formation (Fig. 4), but does not produce cracking, suggests that local hydraulic pressure is the main process responsible for destruction, since it can be quickly relieved by flow of water into neighbouring partially empty pores.

Kipkie *et al.* [19] discusses the difficulties in interpreting cooling–length change experiments unambiguously. We believe the DMR method to be a valuable tool when used in conjunction with other methods to investigate phase transitions in adsorbates.

Acknowledgements

The financial support of the Danish Government Fund for Scientific and Industrial Research is gratefully acknowledged.

References

1. A. S. NOWICK and B. S. BERRY, "Anelastic Relaxation in Crystalline Solids" (Academic Press, New York and London, 1972).
2. I. M. WARD, "Mechanical Properties of Solid Polymers" (Wiley-Interscience, New York, 1971).
3. F. RADJY, Tech. Report No. 90, Dept. of Civil Engineering, Stanford University (1968).
4. F. RADJY and C. W. RICHARDS, *Materials and Structures* **2** (1969) 17.
5. R. A. HELMUTH, Tech. Report No. 154, Dept. of Civil Engineering, Stanford University (1972).
6. F. RADJY and E. J. SELLEVOLD, *Nature Phys. Sci.* **241** (1973) 133.
7. *Idem,* Proceedings of the International Symposium RILEM/IUPAC, Final Report, Vol. IV, Prague (1974) p. C-189.
8. F. RADJY, to be published.
9. G. G. LITVAN, *J. Colloid Interface Sci.* **38** (1972) 75.
10. *Idem, Canad. J. Chem.* **44** (1966) 2617.
11. A. A. ANTONIEU, *J. Phys. Chem.* **68** (1964) 2754.
12. R. F. FELDMAN, *Canad. J. Chem.* **48** (1970) 287.
13. R. DUFAY, I. PRIGOGINE, A. BELLEMANS and D. H. EVERETT, "Surface Tension and Adsorption" (Wiley, New York, 1966).

14. D. H. EVERETT and J. M. HAYNES, *Bulletin RILEM*, no. 27, (1965) 31.
15. Y. MORIOKA, J. KOBAYASHI and I. HIGUCHI, *J. Colloid Interface Sci.* **42** (1973) 156.
16. R. T. PEARSON and W. DERBYSHIRE, *ibid* **46** (1974) 232.
17. G. G. LITVAN, *J. Colloid Interface Sci.* **45** (1973) 154.
18. J. J. BEAUDOIN and C. MacINNES, *Cement and Concrete Res.* **4** (1974) 139.
19. W. B. KIPKIE, R. McINTOSH and B. KELLY, *J. Colloid Interface Sci.* **38** (1972) 3.

Received 31 December 1975 and accepted 30 March 1976.